Improving Melanoma Classification by Integrating Genetic and Morphologic Features

Amaya Viros[1], Jane Fridlyand[2,3], Juergen Bauer[1], Konstantin Lasithiotakis[4], Claus Garbe[4], Daniel Pinkel[2,5], Boris C. Bastian[1,2,6*]

1 Department of Dermatology, University of California San Francisco, San Francisco, California, United States of America, **2** University of California San Francisco (UCSF) Comprehensive Cancer Center, University of California San Francisco, San Francisco, California, United States of America, **3** Department of Epidemiology and Biostatistics, University of California San Francisco, San Francisco, California, United States of America, **4** Department of Dermatology, University of Tübingen, Tübingen, Germany, **5** Department of Laboratory Medicine, University of California San Francisco, San Francisco, California, United States of America, **6** Department of Pathology, University of California San Francisco, San Francisco, California, United States of America

Funding: Supported by grants from the National Cancer Institute (P01 CA025874, R01 CA094963). The funding agency did not have a role in study design, data collection and analysis, decision to publish, or preparation of the manuscript.

Competing Interests: The authors have declared that no competing interests exist.

Academic Editor: Jonathan Rees, University of Edinburgh, United Kingdom

Citation: Viros A, Fridlyand J, Bauer J, Lasithiotakis K, Garbe C, et al. (2008) Improving melanoma classification by integrating genetic and morphologic features. PLoS Med 5(6): e120. doi:10.1371/journal.pmed.0050120

Received: November 20, 2007
Accepted: April 22, 2008
Published: June 3, 2008

Abbreviations: ALM, acral lentiginous melanoma; CSD, chronic sun-induced damage; LMM, lentigo maligna melanoma; NC, not classifiable; NM, nodular melanoma; OR, odds ratio; RGP, radial growth phase; SSM, superficial spreading melanoma; WHO, World Health Organization

* To whom correspondence should be addressed. E-mail: bastian@cc.ucsf.edu

ABSTRACT

Background

In melanoma, morphology-based classification systems have not been able to provide relevant information for selecting treatments for patients whose tumors have metastasized. The recent identification of causative genetic alterations has revealed mutations in signaling pathways that offer targets for therapy. Identifying morphologic surrogates that can identify patients whose tumors express such alterations (or functionally equivalent alterations) would be clinically useful for therapy stratification and for retrospective analysis of clinical trial data.

Methodology/Principal Findings

We defined and assessed a panel of histomorphologic measures and correlated them with the mutation status of the oncogenes *BRAF* and *NRAS* in a cohort of 302 archival tissues of primary cutaneous melanomas from an academic comprehensive cancer center. Melanomas with *BRAF* mutations showed distinct morphological features such as increased upward migration and nest formation of intraepidermal melanocytes, thickening of the involved epidermis, and sharper demarcation to the surrounding skin; and they had larger, rounder, and more pigmented tumor cells (all *p*-values below 0.0001). By contrast, melanomas with *NRAS* mutations could not be distinguished based on these morphological features. Using simple combinations of features, *BRAF* mutation status could be predicted with up to 90.8% accuracy in the entire cohort as well as within the categories of the current World Health Organization (WHO) classification. Among the variables routinely recorded in cancer registries, we identified age < 55 y as the single most predictive factor of *BRAF* mutation in our cohort. Using age < 55 y as a surrogate for *BRAF* mutation in an independent cohort of 4,785 patients of the Southern German Tumor Registry, we found a significant survival benefit ($p < 0.0001$) for patients who, based on their age, were predicted to have *BRAF* mutant melanomas in 69% of the cases. This group also showed a different pattern of metastasis, more frequently involving regional lymph nodes, compared to the patients predicted to have no *BRAF* mutation and who more frequently displayed satellite, in-transit metastasis, and visceral metastasis ($p < 0.0001$).

Conclusions

Refined morphological classification of primary melanomas can be used to improve existing melanoma classifications by forming subgroups that are genetically more homogeneous and likely to differ in important clinical variables such as outcome and pattern of metastasis. We expect this information to improve classification and facilitate stratification for therapy as well as retrospective analysis of existing trial data.

The Editors' Summary of this article follows the references.

Introduction

Cutaneous melanomas can vary significantly in their clinical and histopathological appearance, which has lead to the development and refinement of morphologically based classification systems. The current World Health Organization (WHO) classification of skin tumors [1], which is an extension of the revised Sydney classification from 1986 [2–4], distinguishes four main types of melanoma; superficial spreading melanoma (SSM), lentigo maligna melanoma (LMM), nodular melanoma (NM), and acral lentiginous melanoma (ALM). These distinctions are based on the observation that certain combinations of morphological features of the microscopic growth pattern of melanoma during its early progression phase are associated with clinical features such as anatomic site of the primary tumor, pace of tumor evolution, and patient age. Although these proposed categories undoubtedly represent prototypical instances or archetypes of the clinical and histopathological presentations that are valuable for teaching purposes, their impact on clinical management has been limited. A major reason is that no significant difference in overall survival or treatment responses could be demonstrated between the categories when tumors of equivalent tumor thickness were compared or after metastasis had occurred [5]. Furthermore, these subtypes are defined by multiple criteria, each assessing complex morphological patterns, resulting in a wide range of possible presentations. Thus a considerable portion of melanomas are differentially classified by multiple observers, or are classified as "ambiguous" [6]. Some have questioned the existence of biologically distinct melanoma types altogether, proposing that the morphological differences are entirely secondary to the anatomic site in which the tumor arises [7], or, in the case of NM, are a consequence of differences in the pace of tumor evolution [8].

In order to establish whether a disease is composed of distinct subtypes it is necessary to integrate clinicopathological features with the underlying biologic factors and identify disease groups that are homogeneous in their etiology, clinical behavior, and management requirements. These subtypes, if found, would then form the basis of a clinically useful classification system. In cancer, genetic alterations can serve as biomarkers for classification purposes, in particular if they are causally linked to the disease process. With the advent of therapeutics targeted to genes and signaling pathways, these oncogenic mutations are gaining direct importance for clinical management. But knowledge of the critical constitutional and somatic genetic factors is currently incomplete. Since the clinical characteristics of a tumor must be, at least in part, genetically determined, elucidation of the phenotypic consequences of currently known genetic factors will reveal aspects of their function and highlight gaps in knowledge, which may guide future discovery. More immediately, clinicopathological features that are associated with specific genetic factors provide an attractive basis on which to build a refined classification system that is practical to implement and useful for patient management.

Recently, we described distinct patterns of chromosomal aberrations and mutations in oncogenes such as *BRAF* and *KIT* that correlated more with the site of the primary tumor and the degree of chronic sun-induced damage of the surrounding skin than with the traditional melanoma types [9–13]. Epidemiological studies have independently emphasized the impact of chronic sun exposure on the mole count and survival time of melanoma patients [14,15]. Together, these findings strongly support the existence of distinct melanoma subtypes, but also indicate that these are insufficiently captured by the existing classification system. Using previously recognized morphological features of primary melanoma, we performed a detailed phenotypic characterization of a large cohort of primary melanomas and correlated those features with the mutation status of *BRAF* and *NRAS*, the most commonly mutated oncogenes known in melanoma. Specifically, we defined simple histomorphologic features that can be reproducibly scored in routinely stained sections.

Methods

Tumor Specimens and Mutation Analysis

A total of 302 cases of primary cutaneous melanoma that have been part of previous genetic analyses were included in this study [12,16]. *BRAF* mutation data of exon 15, which includes codon 600, were available from all samples. *NRAS* mutation data of exons 1 and 2 for samples were available from a previously published subset of the samples [12], and were obtained for the remainder of the cases using our standard protocols [17]. For all cases, *NRAS* was only analyzed in melanomas in which no *BRAF* exon 15 mutations were found because earlier studies indicated a very low rate of cooccurrence of these aberrations.

Histopathological Analysis

All histopathological evaluations were carried out on routinely stained HE sections, processed through the UCSF Dermatopathology Service. Cases were classified into SSM, LMM, NM, and, ALM according to the WHO classification, or not classifiable (NC) if they did not fit unequivocally in any of these categories [2,3,18]. The cases were also classified into acral melanoma, and melanoma arising on skin with or without evidence of chronic sun-induced damage (CSD and non-CSD, respectively), as described previously [12].

Analysis of Elementary Histological Features

All sections of tissue that were available for each specimen were examined, and a semiquantitative assessment of each histological feature for a tumor was obtained from the combined analysis of all of the sections. Except where stated otherwise, the morphologic assessments were made in areas of radial growth, excluding areas of vertical growth. Radial growth phase (RGP) and vertical growth phase (VGP) were defined as described by Clark and Elder [19]. For melanomas that were classified as NMs in the WHO classification applying the three-rete ridge rule, the assessment was made in any small intraepidermal component adjacent to the nodular portion wherever possible. NMs without a small adjacent intraepidermal component were not assessed for these features. The histological features examined were as follows.

Upward scatter of intraepidermal melanocytes. The proportion of intraepidermal melanocytes present above the basal layer, irrespective of whether suprabasal melanocytes were arranged singly or as nests, was graded from 0 to 3

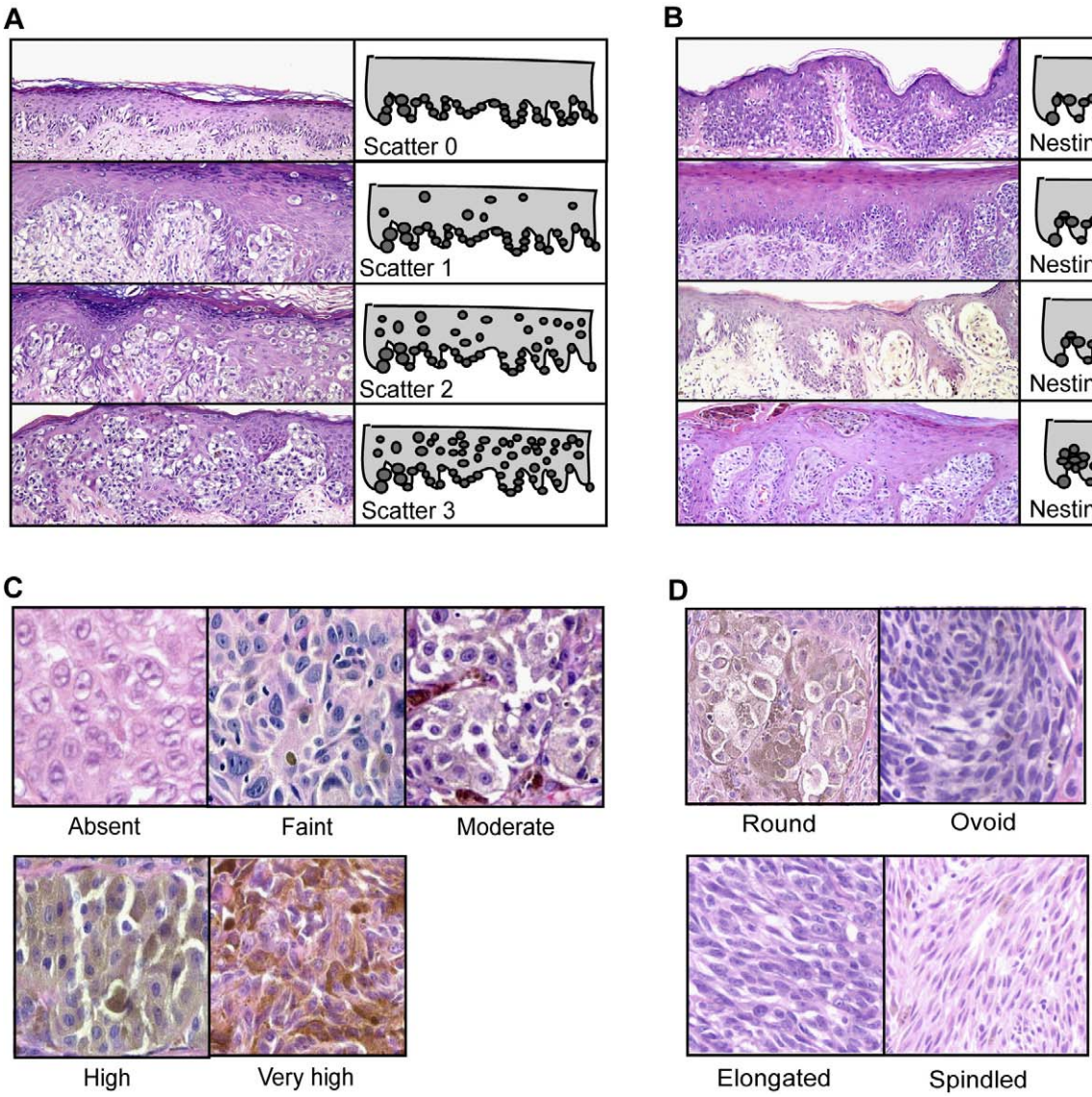

Figure 1. Grading of Morphological Features

(A) Scatter of intraepidermal melanocytes.
(B) Nesting of intraepidermal melanocytes.
(C) Cytoplasmic pigmentation of neoplastic melanocytes.
(D) Cell shapes.
doi:10.1371/journal.pmed.0050120.g001

(Figure 1A) using the following criteria: 0, essentially all melanocytes situated at the dermo-epidermal junction, with only rare melanocytes in higher epidermal layers; 1, the majority of melanocytes (75%–100%) situated at the dermo-epidermal junction, with some present in higher epidermal layers; 2, roughly equal proportions of intraepidermal melanocytes present at the dermo-epidermal junction and in higher epidermal layers; 3, most (>50%) of the intraepidermal melanocytes situated in the upper layers of the epidermis

Nest formation of intraepidermal melanocytes. Intraepidermal melanocytes were defined as arranged in nests rather than single cells if they formed clusters of five or more cells no matter where they were located, e.g., whether within the basal epidermis or in higher layers of the epidermis (Figure 1B). The degree of nesting was quantified as: 0, intraepidermal melanocytes present almost exclusively as single cells with only rare nests; 1, intraepidermal melanocytes predominantly arranged as single cells with no more than 25% of cells in nests; 2, 25%–50% of the intraepidermal melanocytes in nests; 3, >50% of the intraepidermal melanocytes in nests.

Pigmentation of melanocytes. Pigmentation was defined as melanin accumulation within the constituent melanocytes and was scored on a five-point scale using 20× and 40× objectives (Figure 1C). Melanophages were not considered. Pigmentation was assessed in three different ways: maximum pigmentation anywhere in the tumor; average pigmentation across all sections of the RGP; and average pigmentation across all sections of the vertical growth phase (VGP). These

parameters gave similar results in the final analysis (Table S1), so we standardized on using the maximum pigmentation scored anywhere in the tumor. Pigmentation was scored from 0–4 using the scale: 0, (absent) no pigment discernible even at high power; 1, (faint) pigmentation barely visible at low power. At high power, melanocytes showed a faint diffuse melanin pigment or a few pigment granules. 2, (moderate) pigmentation visible at low power with translucent cytoplasm that is significantly lighter than the hematoxylin stained nuclei; 3, (high) pigmentation easily visible at low power with the cytoplasmic pigmentation reaching an intensity approximating that of the nucleus; 4, (very high) cytoplasm strikingly pigmented making it difficult to identify nuclei.

Epidermal contour. The contour of the epidermis involved by the RGP of the melanoma was compared to the adjacent normal epidermis (Figure S1A) and scored from 0 to 4: 0, (atrophic) markedly thinned epidermis with effacement of rete ridges; 1, (thinned) thinned epidermis with partial attenuation of rete ridges; 2, (normal) epidermal silhouette similar to the adjacent uninvolved epidermis; 3, (thickened) slight to moderate epidermal hyperplasia with elongation of the rete ridges resulting in a maximum 2-fold increase in epidermal thickness; 4, (hyperplastic) marked epidermal hyperplasia resulting in a greater than 2-fold increase in epidermal thickness.

Lateral circumscription. Lateral circumscription was assessed by examining the transition of the intraepidermal growth portion of the tumor to normal skin at the tumor periphery. The area with the most gradual transition in any of the tissue pieces (Figure S1B) was scored from 0 to 2. 0, (discontinuous) areas of apparently uninvolved epidermis interspersed with tumor. Areas of uninvolved epidermis apparently caused by regression were considered tumor; 1, (gradual but continuous) continuous decrease of the number of intraepidermal melanocytes making it difficult to pinpoint the transition to normal skin to within one or two rete ridges or 0.1 mm; 2, (abrupt) transition from involved epidermis to the adjacent normal skin easily determined within one or two rete ridges or 0.1 mm.

Solar elastosis. The degree of solar elastosis was classified on an 11-category scale ranging from 0 to 3+ by examining the normal skin surrounding the melanoma using the 10× and 20× lenses, as described previously [16].

Size and shape of cells, nuclei, and nucleoli. Size and shape of tumor cells and their nuclei were assessed in the most cellular portion of the tumor using a 20× lens. Nuclei of small lymphocytes, which we determined ranged in size from 4 to 5 μm, were used as a size reference. Visual assessment of size was quantified on a scale from 1 to 3. Tumor cells were considered 1, small; 2, medium; or 3, large, if the greatest diameter was <8 μm, between 8 and 10 μm, and >10 μm, respectively (Figure S1C). Similarly, nuclei were considered 1, small; 2, medium; and 3, large, if the greatest diameter was <5 μm, between 5 and 6 μm, and >6 μm. Nucleolar size was assessed in the most cellular portion of the tumor using a 40× lens: 1, (small) nucleoli of tumor cells smaller than those of keratinocytes, or not discernible; 2, (medium) tumor nucleoli comparable in size to those of keratinocytes; 3, (large) tumor nucleoli larger than those of keratinocytes.

Cell shape was visually assessed at 20× in the most cellular portion of the tumor using (Figure 1D). The visual assessment graded the cells from 0 to 3: 0, (round) long and short diameters approximately equal; 1, (ovoid) long diameter approximately one-third greater than the short diameter; 2, (elongated) long diameter between one-third and two times longer than the short diameter; 3, (spindled) long diameter >two times the short diameter.

Sizes and shapes of cells were also determined quantitatively in 264 samples of the cohort using photomicrographs taken with a 20× lens and averaging ten random cells within a representative area (Table S2). Sizes were expressed as the product of the long and short diameter (μ^2), and shapes as their ratio. Quantitative and visual measurements showed good agreement (Kendall's Tau Test 0.4–0.6) (Table S3). The visual assessments were used in the analysis, as discussed below.

Ulceration. Ulceration was defined as the presence of a full-thickness epidermal defect; evidence of host response (i.e., fibrin deposition, neutrophils); and thinning, effacement, or reactive hyperplasia of the surrounding epidermis [20].

Thickness. Tumor thickness was measured in millimeters according to Breslow [21].

Statistical Analysis

The univariate analyses for binary outcomes (e.g., *BRAF* mutation present or not) were performed by fitting a logistic regression with each of the measurements. Standard error of the odds ratio (OR) was determined using the Taylor expansion rule. All ordinal measurements of the phenotypic characteristics were treated as scores in the analyses after testing for linearity of the scores with respect to each outcome. Where nonlinear, the polynomials of higher order were fitted to correct nonlinearity according to the default approach to treatment of ordinal variables. Continuous variables (thickness, cell size, cell shape, nuclear size, and nuclear shape) were preprocessed by adding one-tenth of the smallest nonzero value of the respective variable followed by taking log10 of the values to render their distribution more normal. The unordered categorical variables (anatomic site, WHO type, non-CSD, CSD, Acral grouping [11], and gender) were treated as factor variables in logistic regression. Multivariate analyses to predict mutation status were performed using single binary classification tree classifiers [22], Random Forests [23], and multivariate logistic regression. A detailed description of the methods is provided in the Text S1. All statistical analyses were conducted using the freely available R statistical language.

Results

Morphometric Analysis of Phenotypic Features

Clinical information, *BRAF* mutation status, and WHO classifications of all 302 primary cutaneous melanomas in this study are summarized in Table 1. The phenotypic characteristics that we focused on in our measurements comprised "elementary" features that mostly are combined in various ways in the WHO classification. For example, in the WHO classification the features "lentiginous" and "pagetoid" growth are prominently used as opposing ends of a spectrum of intraepidermal growth. However, both lentiginous and pagetoid are "complex" patterns composed of several separable features including (a) whether the neoplastic melanocytes are scattered throughout all layers of the epidermis (in pagetoid) or are situated in the basal layer (in

Table 1. Clinical Characteristics of Patients and Melanomas by Mutation Status of *BRAF* and *NRAS* Included in Our Analysis

Clinical Characteristics	Category	*n* (%)	*BRAF* Mutation, *n* (%)	*NRAS* Mutation *n* (%)	Neither Mutation *n* (%)
WHO subtype	**SSM**	189 (62.6)	98 (51.9)	36 (19)	55 (29.1)
	LMM	39 (12.9)	13 (33.3)	4 (10.3)	22 (56.4)
	ALM	23 (7.6)	3 (13)	2 (8.7)	18 (78.3)
	NM	16 (5.3)	11 (68·8)	2 (12.5)	3 (18.7)
	NC	35 (11.6)	17 (48·6)	6 (17.1)	12 (34.3)
	Total	302 (100)	142 (47)	50 (16.6)	110 (36.4)
Acral, CSD, non-CSD grouping	**Non-CSD**	152 (50.3)	96 (63·1)	27 (17.8)	29 (19.1)
	CSD	106 (35.1)	33 (31·1)	17 (16.1)	56 (52.8)
	Acral	40 (13.2)	10 (25)	5 (12.5)	25 (62.5)
	NC	4 (1.3)	3 (75)	1 (25)	0
	Total	302 (100)	142 (47)	50 (16.6)	110 (36.4)
Anatomic site	**Face/Scalp**	48 (15.9)	14 (29.2)	5 (10.4)	29 (60.4)
	Trunk	114 (37.7)	72 (63.2)	17 (14.9)	25 (21.9)
	Upper Ext	37 (12.3)	13 (35.1)	10 (27.1)	14 (37.8)
	Lower Ext	52 (17.2)	28 (53.8)	12 (23.1)	12 (23.1)
	Acral	35 (11.6)	8 (22.9)	4 (11.4)	23 (65.7)
	Total	286 (94.7)	135 (47.2)	48 (16.8)	103 (36)
Sex	**Female**	128 (42.4)	69 (53.9)	21 (16.4)	38 (29.7)
	Male	154 (51)	66 (42.8)	24 (15.6)	64 (41.6)
	Total	282 (93.4)	135 (47.9)	45 (15.9)	102 (36.2)
Age (y)	—	59.5 (26)[a]	51 (24.5)[a]	63 (25.5)[a]	66 (18)[a]
Thickness (mm)	—	1.2 (2.4)[a]	1 (1.7)[a]	1.1 (1.6)[a]	1.6 (2.8)[a]

Values are expressed as *n* (%) unless otherwise noted. Total percentages that do not add up to 100% have missing values.
[a]Median and interquartile range.
doi:10.1371/journal.pmed.0050120.t001

lentiginous); (b) whether the cells are arranged partially in nests (in pagetoid) or predominantly as single units (in lentiginous); and (c) whether the melanocytes are enlarged and round (in pagetoid) or small with scalloped contours or spindled (in lentiginous). Therefore to describe intraepidermal growth we defined and assessed features termed: scatter, nest formation, size and shape (Figure 1). Similar to the WHO classification, we focused our evaluation of the features primarily on the early progression phases, e.g., the RGP of the tumor in the expectation that this would be the most informative regarding its "histogenetic" origin.

All features were visually scored in the 302 tumors by one of us (AV). Interobserver agreement was determined by having an additional observer (JB) score a randomly selected subset of 50 cases. The scorers were blinded to knowledge of the genetic status of the tumors until the scoring was complete. Kappa statistics [24] indicated moderate to excellent agreement (Table S4). Table 2 shows the number of tumors by phenotypic feature and mutation status. Figure 2 shows a heatmap of features by mutation status (Figure 2A) and by the WHO subtypes (Figure 2B).

BRAF, but Not *NRAS*, Mutation Status Is Strongly Related to Some Phenotypic Features

Tables 3 and S5 show the results of univariate analysis to determine the association statistic between the elementary phenotypes and mutation status. Several are highly significant. Since most of the features are assessed as ordinal variables, the ORs reflect the increase (or decrease) of the odds per unit increment. For example in the comparison of nesting between melanomas with and without *BRAF* mutations (first column), the OR of 3.11 indicates the increase in odds for one increment of the ordinal scale for scatter (e.g., nesting 1 to nesting 2). To calculate the odds for an increment of two the indicated OR should be squared. Compared to melanomas without *BRAF* mutations, melanomas with *BRAF* mutations showed statistically significantly higher degrees of intraepidermal scatter of melanocytes, and a higher proportion of melanocytes arranged in nests. In addition, the epidermis of the RGP of melanomas with *BRAF* mutations was more commonly thickened compared to the surrounding skin, i.e., the score for the "epidermal contour" had a higher average value, and the transition from the tumor into the surrounding skin tended to be more abrupt than in melanomas without *BRAF* mutations, i.e., "lateral circumscription" had a higher average score. Furthermore, the tumor cells of *BRAF*-mutated melanomas were larger, had a rounder shape, and showed a higher degree of pigmentation than cells in tumors without *BRAF* mutations. As we reported previously [16], melanomas with *BRAF* mutations also had a lower degree of solar elastosis in the surrounding skin than melanomas without *BRAF* mutations.

Given the significant univariate correlations, we employed several multivariate statistical approaches to define the most powerful combinations of variables for prediction of mutation status. These analyses produced a consistent set of variables that included the morphological features pigmentation, upward scatter, nesting of intraepidermal melanocytes, and cell shape. In addition, a younger age at diagnosis was independently associated with *BRAF* mutation status (Table S6). The results of the multivariate analyses are most intuitively displayed using a binary classification tree since it defines a decision structure using specific thresholds for individual characteristics at each node. Classification trees developed using all clinical and morphologic variables correctly predicted *BRAF* mutation status with up to 82% accuracy if one required a prediction for all tumors. Classification trees with high prediction accuracy also formed

Table 2. Morphologic Features of Melanomas by Mutation Status of *BRAF* and *NRAS* Included in Our Analysis

Morphological Characteristics	Category	*n* (%)	*BRAF* Mutation, *n* (%)	*NRAS* Mutation, *n* (%)	Neither Mutation, *n* (%)
Scatter	**Absent**	71 (23.5)	3 (2.1)	22 (44)	46 (41.8)
	Slight	112 (37.1)	59 (41.6)	18 (36)	35 (31.8)
	Medium	54 (17.9)	36 (25.3)	5 (10)	13 (11.8)
	Prominent	31 (10.2)	26 (18.3)	0	5 (4.61)
	Total assessable	268 (88.7)	124 (87.3)	45 (90)	99 (90)
Pigmentation	**Absent**	56 (18.5)	12 (8.4)	9 (18)	35 (31.8)
	Slight	63 (20.9)	18 (12.7)	18 (36)	27 (24.5)
	Medium	76 (25.2)	37 (26.1)	11 (22)	28 (25.5)
	High	59 (19.5)	38 (26.8)	7 (14)	14 (12.7)
	Very high	42 (13.9)	34 (23.9)	2 (4)	6 (5.5)
	Total assessable	296 (98)	139 (97.9)	47 (94)	110 (100)
Nesting	**Absent**	32 (10.6)	0	9 (18)	23 (20.9)
	Slight	59 (19.5)	20 (14.1)	11 (22)	28 (25.5)
	Medium	81 (26.8)	32 (22.5)	12 (24)	37 (33.6)
	Prominent	96 (31.8)	72 (50.7)	13 (26)	11 (10)
	Total assessable	268 (88.7)	124 (87.3)	45 (90)	99 (90)
Circumscription	**Abrupt**	122 (40.4)	79 (55.7)	14 (28)	29 (26.4)
	Continuous	90 (29.8)	34 (23.9)	18 (36)	38 (34.6)
	Discontinuous	31 (10.3)	5 (3.5)	10 (20)	16 (14.5)
	Total assessable	243 (80.5)	118 (83.1)	42 (84)	83 (75.5)
Epidermal contour	**Atrophy**	6 (2)	0	2 (4)	4 (3.6)
	Effacement	28 (9.3)	11 (7.8)	6 (12)	11 (10)
	Normal	41 (13.6)	16 (11.2)	8 (16)	17 (15.5)
	Thickening	104 (34.4)	53 (37.3)	18 (36)	33 (30)
	Hyperplasia	82 (27.1)	41 (28.9)	10 (20)	31 (28.2)
	Total assessable	261 (86.4)	121 (85.2)	44 (88)	96 (87.3)
Solar elastosis [1–11]	**—**	6 (4)[a]	5 (3)[a]	6 (4)[a]	7 (3)[a]
Cell size[b]	**Small**	141 (46.7)	53 (37.3)	34 (68)	54 (49)
	Medium	117 (38.7)	67 (47.2)	11 (22)	39 (35.5)
	Large	38 (12.6)	21 (14.8)	4 (8)	13 (11.8)
	Total assessable	296 (98)	141 (99.3)	49 (98)	106 (96.4)
Cell shape [b]	**Round**	197 (65.2)	110 (77.5)	29 (58)	58 (52.7)
	Ovoid	45 (14.9)	16 (11.3)	8 (16)	21 (19.1)
	Elongated	35 (11.6)	11 (7.7)	7 (14)	17 (15.5)
	Spindled	19 (6.3)	4 (2.8)	5 (10)	10 (9.1)
	Total assessable	296 (98)	141 (99.3)	49 (98)	106 (96.4)
Nuclear size [b]	**Small**	200 (66.2)	87 (61.3)	39 (78)	74 (67.3)
	Medium	87 (28.8)	49 (34.5)	10 (20)	28 (25.5)
	Large	8 (2.6)	4 (2.8)	0	4 (3.6)
	Total assessable	295 (97.7)	140 (98.6)	49 (98)	106 (96.4)
Nuclear shape [0–1]	**—**	0.74 (0.16)[a]	0.76 (0.1)[a]	0.69 (0.25)[a]	0.71 (0.2)[a]
Nucleolar size	**Small**	60 (19.9)	24 (16.9)	10 (20)	26 (23.6)
	Medium	145 (48)	77 (54.2)	22 (44)	46 (41.8)
	Large	96 (31.8)	41 (28.9)	18 (36)	37 (33.7)
	Total assessable	301 (99.7)	142 (100)	50 (100)	109 (99.1)
Ulceration	**Yes**	94 (31.1)	40 (28.2)	12 (24)	42 (38.2)
	No	201 (66.6)	100 (70.4)	36 (72)	65 (59.1)
	Total assessable	295 (97.7)	140 (98.6)	48 (96)	107 (97.3)

Values are expressed as *n* (%) unless otherwise noted. Total percentages that do not add up to 100% have missing values.
[a]Median and interquartile range.
[b]Variables for which continuous measurements were also assessed (Table S2).
doi:10.1371/journal.pmed.0050120.t002

when only morphologic features were included in the model. Figure 3A shows one such tree, which has 76% accuracy for predictions for all samples. However, it is clear that some branches of the tree lead to much stronger predictions than others. Thus tumors without "upward scatter" have a very low probability of being *BRAF* mutant, while those with "scatter" > 0 and "nesting" > 2 are almost all *BRAF* mutant. However, tumors with "scatter" > 0 but lower "nesting" have about equal chance of being *BRAF* wild-type (47%) or mutant (53%), with high "pigmentation" increasing the odds of being mutant to 70%.

Although intuitive to interpret, single classification trees are inherently unstable in the sense that slight perturbations in the dataset used for tree building may lead to large changes in the tree topology, e.g., several trees with approximately the same discrimination power can be found. Resampling-based algorithms are well-known solutions for improving the accuracy of single classification trees. We used the Random Forest classifier, a method that grows many classification trees, each based on a different subset containing on average 66% of the samples. The resulting collection of individual trees is referred to as "random forest." The final prediction for each sample is the outcome of the majority vote of those trees in the forest that did not include that sample in their

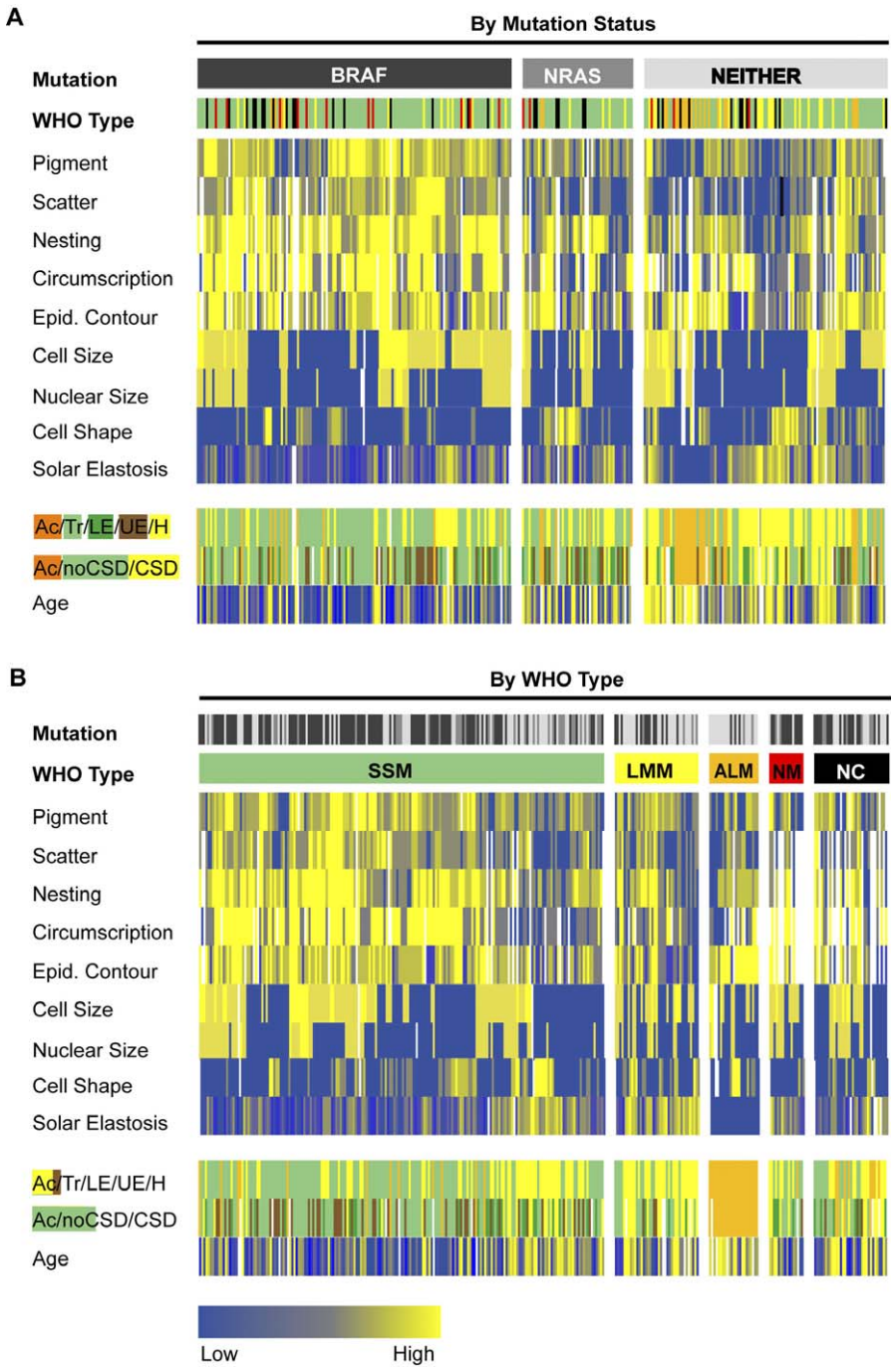

Figure 2. Heatmap of Features by Mutation Status (A) and by WHO Subtypes (B)

Variables significantly associated with *BRAF*. Samples are in columns, variables in rows. The scores range from shades of blue (low score), to gray (intermediate scores), to yellow (high scores). Samples are ordered within each category using agglomerative hierarchical clustering on morphological variables by Euclidean distance and Ward's criterion. Ac, acral; CSD, chronic sun damage as defined in [12]; H, head; LE, lower extremity; Tr, trunk; UE, upper extremity;.

doi:10.1371/journal.pmed.0050120.g002

development. The unbiased estimate of the error is given by 1, prediction accuracy [23,25]. As expected, random forests significantly improved the classification performance, correctly predicting *BRAF* status with 91.8% accuracy using all variables, and 87% using morphological variables only. In comparison, the probability for predicting *BRAF* mutation in this dataset by chance is about 50%. Thus the conventional morphological parameters of a tumor are substantially affected by *BRAF* mutations. The performances of the different classification approaches we applied are summarized in Table S6.

While the elementary morphological characteristics that contribute to the WHO classification system have a very strong relationship to *BRAF* mutation status, the WHO

Table 3. Comparison of Morphological Variables Depending on the Mutation Status of *BRAF* and *NRAS*

Criteria	Category	*BRAF* Mutant Versus *BRAF* Wild-Type		*BRAF* Mutant Versus Neither Mutant		*BRAF* Mutant Versus *NRAS* Mutant		*NRAS* Mutant Versus Neither	
		OR (CI 95%)	*p*-Value	OR (CI 95%)	*p*-Value	OR (CI 95%)	*p*-Value	OR (CI 95%)	*p*-Value
Scatter	**Linear**[a]	27.95 (10.10–77.37)	<0.0001	21.08 (7.55–58.77)	<0.0001	8.1 (3.81–17.1)	<0.0001	0.79 (0.5–1.25)	0.32
	Quadratic[a]	0.32 (0.14–0.73)	0.007	0.27 (0.12–0.63)	0.002				
	Cubic[a]	1.96 (1.12–3.45)	0.02	1.91 (1.04–3.52)	0.038				
Pigmentation	—	2.01 (1.63–2.48)	<0.0001	2.01 (1.61–2.52)	<0.0001	1.94 (1.44–2.61)	<0.0001	1.09 (0.81–1.45)	0.58
Nesting	—	3.11 (2.27–4.27)	<0.0001	3.68 (2.55–5.31)	<0.0001	2.44 (1.65–3.61)	<0.0001	1.32 (0.93–1.88)	0.13
Circumscription	—	3.06 (2.01–4.67)	<0.0001	2.99 (1.88–4.75)	<0.0001	3.25 (1.87–5.64)	<0.0001	0.89 (0.54–1.48)	0.66
Epidermal contour	—	1.3 (1.02–1.66)	0.031	1.25 (0.96–1.63)	0.098	1.47 (1.04–2.07)	0.028	0.89 (0.65–1.21)	0.45
Solar elastosis	—	0.89 (0.81–0.97)	0.006	0.88 (0.8–0.96)	0.006	0.88 (0.77–1.02)	0.08	0.97 (0.87–1.08)	0.6
Cell size	—	1.63 (1.16–2.28)	0.004	1.4 (0.97–2.03)	0.08	2.51 (1.44–4.38)	0.001	0.59 (0.34–1.02)	0.06
Cell shape	—	0.58 (0.44–0.76)	<0.0001	0.57 (0.42–0.77)	0.0002	0.61 (0.43–0.87)	0.006	0.96 (0.69–1.33)	0.79
Nuclear size	—	1.48 (0.96–2.29)	0.076	1.26 (0.79–2.01)	0.34	2.39 (1.14–5.02)	0.02	0.56 (0.27–1.18)	0.13
Nuclear shape[b]	—	1.66 (1.23–2.25)	0.001	1.63 (1.16–2.27)	0.004	1.51 (1.05–2.17)	0.02	0.96 (0.67–1.38)	0.82
Nucleolar size	—	1 (0.73–1.4)	0.99	1.04 (0.73–1.48)	0.83	0.92 (0.57–1.47)	0.72	1.11 (0.71–1.74)	0.64
Ulceration	—	0.75 (0.46–1.23)	0.25	0.62 (0.36–1.06)	0.07	1.2 (0.57–2.54)	0.63	0.52 (0.24–1.1)	0.08
WHO subtype	**SSM**	1 (Reference)	<0.0001	1 (Reference)	<0.0001	1 (Reference)	0.84	1 (Reference)	0.02
	LMM	0.46 (0.23–0.96)	0.037	0.33 (0.15–0.71)	0.004	1.19 (0.37–3.9)	0.77	0.28 (0.09–0.87)	0.03
	ALM	0.14 (0.04–0.48)	0.002	0.09 (0.03–0.33)	0.0002	0.55 (0.09–3.43)	0.52	0.17 (0.04–0.78)	0.02
	NM	2.04 (0.68–6.11)	0.2	2.06 (0.55–7.69)	0.28	2.02 (0.43–9.56)	0.38	1.02 (0.16–6.4)	0.98
	NC	0.88 (0.43–1.8)	0.72	0.8 (0.35–1.79)	0.58	1.04 (0.38–2.85)	0.94	0.76 (0.26–2.22)	0.62
Acral, CSD, non-CSD Grouping	**Non-CSD**	1 (Reference)	<0.0001	1 (Reference)	<0.0001	1 (Reference)	0.38	1 (Reference)	0.002
	CSD	0.26 (0.16–0.45)	<0.0001	0.18 (0.1–0.32)	<0.0001	0.55 (0.26–1.13)	0.1	0.33 (0.15–0.69)	0.004
	Acral	0.19 (0.09–0.43)	<0.0001	0.12 (0.05–0.28)	<0.0001	0.56 (0.18–1.79)	0.33	0.21 (0.07–0.64)	0.006
	NC	1.75 (0.18–17.23)	0.63	1,739,339 (0–∞)	0.99	0.84 (0.08–8.44)	0.89	2,275,082 (0–∞)	0.99
Gender	**Female**	1	0.06	1	0.03	1	0.61	1	0.28
	Male	0.64 (0.4–1.03)	0.06	0.57 (0.34–0.96)	0.03	0.84 (0.43–1.65)	0.61	0.68 (0.33–1.38)	0.28
Age (y)	—	0.96 (0.94–0.97)	<0.0001	0.95 (0.93–0.97)	<0.0001	0.96 (0.94–0.98)	0.0007	0.99 (0.97–1.01)	0.31
Anatomic site	**Trunk**	1 (Reference)	<0.0001	1 (Reference)	<0.0001	1 (Reference)	0.18	1 (Reference)	0.004
	Face/scalp	0.24 (0.12–0.5)	0.0001	0.17 (0.08–0.37)	<0.0001	0.66 (0.21–2.1)	0.48	0.25 (0.08–0.8)	0.02
	Upper extremity	0.32 (0.15–0.69)	0.004	0.32 (0.13–0.78)	0.01	0.31 (0.12–0.82)	0.02	1.05 (0.38–2.91)	0.92
	Lower extremity	0.68 (0.35–1.32)	0.26	0.81 (0.36–1.83)	0.61	0.55 (0.23–1.3)	0.17	1.47 (0.54–4.04)	0.45
	Acral	0.17 (0.07–0.42)	<0.0001	0.12 (0.05–0.3)	<0.0001	0.47 (0.13–1.75)	0.26	0.26 (0.07–0.87)	0.03
Thickness (mm)	—	0.75 (0.47–1.19)	0.22	0.76 (0.46–1.25)	0.28	0.71 (0.34–1.49)	0.36	0.98 (0.51–1.91)	0.96

[a]As opposed to the other variables tested, for scatter the odds for *BRAF* mutation increased in a nonlinear fashion, with a dramatic increase in odds of being *BRAF* mutant from cases with no scatter (score 0) to slight scatter (score 1). To address this nonlinearity, we also calculated higher order polynomial terms. Note that in the case of scatter the linear term can no longer be interpreted directly as mean OR per incremental unit as exemplified for nesting in the results section.

[b]OR is calculated per decimal point increment. For ordinal and continuous variables, the OR is displayed as mean OR per incremental unit, for categorical variables it is compared to a reference.

CI, confidence interval.

doi:10.1371/journal.pmed.0050120.t003

categories were not independently associated with *BRAF* mutation status since mutations are found in considerable proportions of all WHO categories, with the exception of ALM, Table 1, and Figure 2. The strong relationship of the elementary characteristics to mutation status is emphasized by the fact that the same associations remained significant when the analyses were restricted to individual WHO categories, where the proportion of mutations ranged from 13% in the Acral category to 52% in the SSM category (Table S7). These findings suggest that the elementary features can be combined to a refined classification algorithm yielding melanoma groups that are more homogeneous with regard to their underlying genetic alterations.

In contrast to *BRAF*, a different, much smaller, set of significant criteria was found in univariate comparisons between melanomas with *NRAS* mutations and melanomas with mutations in neither *BRAF* nor *NRAS* (Tables 3 and S2). However, the single tree classifier did not produce any significant splits indicating that the power of these variables to predict *NRAS* mutation status was limited.

We did not have sufficient outcome information of the patients in our cohort to test for differences between the melanoma groups formed by the classification tree of Figure 3A. Since none of the morphological features assessed in our study is currently recorded in any tumor registry we also could not readily apply this approach to existing clinical cohorts. However, gender, patient age, WHO subtype, site of primary tumor, tumor thickness, and presence or absence of ulceration are routinely recorded in registries. Using these variables only on our data, a classification tree consisting of a stump (a tree with only two terminal nodes) was formed with age as the sole criterion for predicting *BRAF* status. Using this tree 69% of the melanomas in patients under the age of 55 y had *BRAF* mutant tumors, while only 35.3 % were *BRAF* mutant in older patients (Figure 3B). Applying this age cutoff to a cohort of 4,785 patients from the German Melanoma Registry [26] significant differences in disease-specific overall survival and disease-free survival were found (Figure 3B). In multivariate analysis, this age cutoff was associated with outcome independent of tumor thickness, anatomic site, and

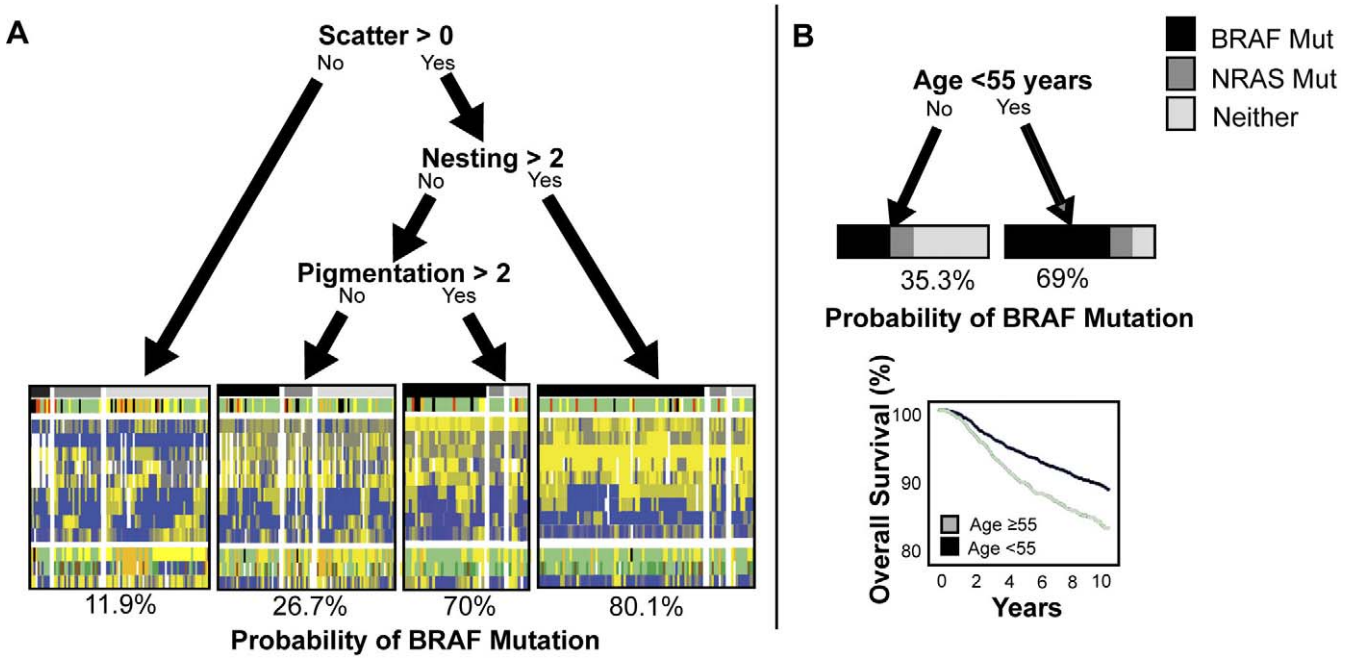

Figure 3. Prediction Algorithms of *BRAF* Mutation

Prediction trees for *BRAF* mutation status with morphologic variables (A) or variables in the Southern German Tumor Registry (B).
(A) Terminal nodes display heatmaps showing samples by mutation status, ordered and coded as in Figure 2A.
(B) The prediction tree for *BRAF* mutation using the variables of age, sex, body site, and WHO type also recorded in melanoma registries identifies an age cutoff of 55 y as the single best predictor of *BRAF* mutation status. Kaplan Meier survival analysis from the Southern German Tumor Registry shows a significant ($p < 0.0001$) decrease in survival when stratified by this age cutoff.
doi:10.1371/journal.pmed.0050120.g003

presence or absence of ulceration. In addition to a better prognosis, the group that, on the basis of their age, was more likely to have a *BRAF* mutant melanoma more frequently presented with metastases to regional nodes; whereas patients that, on the basis of their age, were less likely to have a *BRAF* mutant melanoma tended to have either localized or systemic metastases (Table S8).

Discussion

In this study we demonstrate that histopathological features of the primary tumor, many of which have been part of the WHO classification, provide substantial information on the mutation status of an important melanoma gene, *BRAF*. We found that phenotypic features such as increased upward scatter and nest formation of intraepidermal melanocytes; thickening of the involved epidermis; sharp demarcation from the surrounding skin; as well as the presence of a larger, rounder, and more pigmented tumor cells were distinguishing features of melanomas with *BRAF* mutation. This finding suggests that further research will reveal additional phenotypic associations with other genetic factors, including both germ line constitution of the patient and the somatic alterations in the tumor. In general it is not to be expected that single morphological parameters will be associated with individual genetic factors since it is likely that there will be interactions, or partial or functional redundancy, among them.

Results of genotype-phenotype studies can be applied in two directions. Starting with the genetics, the resulting phenotypes may allow generation of hypotheses concerning the function of a genetic factor. For example, our observation of increased melanin pigment in the tumor cells in melanomas with *BRAF* mutations is in line with recent reports of cooperation between *BRAF* and MITF in melanoma development. MITF is an important transcriptional regulator of pigmentation that is amplified in a subset of melanomas and cooperates with *BRAF* in transforming immortalized human melanocytes [27]. A link between *BRAF* and pigmentation is further supported by a recent independent observation that *BRAF*-mutant melanomas are also more pigmented macroscopically [28]. Our study also identified strong associations between upward scatter of intraepidermal melanocytes and formation of nests and *BRAF* mutation. Upward scatter is unlikely to be entirely attributable to *BRAF* mutations, as scatter is typically absent in nevi, many of which have *BRAF* mutations [29], suggesting that other genes cooperating with *BRAF* may be involved. By contrast, many nevi also show melanocytes arranged in nests and are sharply circumscribed, features that are also more frequent in *BRAF*-mutant melanomas. Studies to determine which of the features found here to be associated with *BRAF* mutant melanomas show similar genotype-phenotype associations in nevi are currently underway.

In the other direction, phenotypic characteristics that are conventionally assessed in the clinic can be used to develop a practical classification system in which the classes are genetically homogeneous, and thus more likely to provide information relevant to patient management. Such a system may provide valuable, outcome-related information from its classes even before the genetic factors of each class are completely understood. Such a classification system is likely

to have an important clinical impact. To achieve this goal the practicability and interobserver reproducibility of the criteria that we defined need to be assessed in a clinical setting and the classification algorithms validated on independent cohorts of cases. Such efforts have been initiated and shown good to excellent interobserver agreements in scoring the features used in this study among expert pathologists (to be published separately).

Among the few variables in our study that overlapped with data recorded in large patient registries, age was the variable that best predicted *BRAF* status. A strong association between patient age at diagnosis and *BRAF* mutation status has been reported previously by us and others [11,28,30,31]. Using the age cutoff of 55 y determined in our experimental cohort, we found a significant difference in disease-specific and relapse-free (unpublished data) survival in an independent clinical cohort of 4,785 patients. Several previous studies including our own [11,30,32–36] have not found significant survival differences between melanomas with and without *BRAF* mutation. However, the numbers of patients in these studies are comparably small, and this simple cutoff may be reflecting currently unknown genetic effects that interact with or substitute for *BRAF* mutations, and thus reveal significantly different clinical behavior. Future studies will be required to better understand the factors involved in this survival difference, hopefully resulting in improved ability to predict the future course of a particular tumor.

The presence of *NRAS* mutations was not strongly associated with the phenotypic measurements we performed. In the univariate analysis the majority of the OR point estimates for association with *NRAS* mutation are close to one, and so if true associations are present we would expect them to be much weaker than for *BRAF*. Multivariate analyses did not significantly enhance the prediction power. This dissimilarity could reflect differences in signaling between *BRAF* and *NRAS*, with *NRAS* having more pleiotropic effects. Larger numbers of cases and additional knowledge of equivalent genetic alterations in melanomas without *BRAF* and *NRAS* mutations are required to evaluate whether some of the features used here and/or others can further increase the discrimination between genetically defined subtypes. We have recently described activation of KIT by mutation and/or copy number increases in mucosal, acral, and CSD melanomas [13]. Too little tissue or DNA was left from the current cohort of cases to test for associations between KIT aberrations and any of our features.

Disease classification evolves from descriptions of a combination of symptoms (syndromes), to more refined definitions that integrate underlying causes. The increase in knowledge of underlying causative genetic alterations in melanoma offers an opportunity to reassess the syndromic classification scheme that emerged from the Sydney classification [3] and its revision [4] into the current WHO classification. The genotype-phenotype correlations discovered in our study testify to the intuition of the originators of the morphological classification scheme. The observation that simple combinations of features could predict *BRAF* mutation status independent of, and even within WHO subtypes, indicates that the morphological criteria we used can be employed to refine the existing classification, providing an opportunity to identify disease subsets that are genetically more homogenous. Our result represents but one step towards improved classification, and we expect it to be modified in light of future discoveries.

In the distant future when genetic knowledge is complete and targeted therapeutic options are numerous, the appropriate clinical work up of a patient is likely to be quite different from current practice. While initial diagnosis and aspects of staging will require histopathology, more subtle distinctions will employ molecular analysis. Reaching this goal requires following a complex, uncertain path of incremental advances built on new discoveries and continuous refinement of perceived relationships among disparate types of knowledge. Here we have investigated the relationship of elementary histopathological characteristics of melanomas to the mutation status of two genes, *BRAF* and *NRAS*. A strong relationship was found for the first but not for the second. As more studies are performed, additional strong genotype-phenotype relationships may be found, more subtle effects of genetic interactions and complementation may be revealed, and consequences of these factors for clinical behavior of individual tumors may be elucidated. As this process unfolds, phenotypic characteristics will become progressively more useful as surrogates for missing genetic knowledge. Thus development of a melanoma classification system that combines analysis of known genetic factors with histopathology may produce a clinically powerful method for managing individual patients and guiding research in the immediate future.

Supporting Information

Alternative Language Abstract S1. Translation of the Abstract into Spanish by A. Viros

Found at doi:10.1371/journal.pmed.0050120.sd001 (29 KB DOC).

Figure S1. Grading of Morphological Features

(A) Epidermal contour, (B) lateral circumscription of tumors, (C) cell size.

Found at doi:10.1371/journal.pmed.0050120.sg001 (1.6 MB JPG).

Table S1. Alternative Assessments of Pigmentation

The data are shown by mutation status of *BRAF* and *NRAS*. The variable of maximum pigmentation was used for statistical analysis and is shown in Tables 1–3. Total percentages that do not add up to 100% have missing values.

Found at doi:10.1371/journal.pmed.0050120.st001 (29 KB DOC).

Table S2. Morphometric Assessment of Cell Size, Cell Shape, and Nuclear Size as a Function of Mutation Status

IQR, interquartile range.

Found at doi:10.1371/journal.pmed.0050120.st002 (28 KB DOC).

Table S3. Concordance between Quantitative and Semiquantitative Measurements of Cell Size and Cellular and Nuclear Shape

Found at doi:10.1371/journal.pmed.0050120.st003 (26 KB DOC).

Table S4. Quadratic Weighted Kappa Coefficient Reflecting Interobserver Agreement between Two Observers Assessed on 50 Samples

Found at doi:10.1371/journal.pmed.0050120.st004 (27 KB DOC).

Table S5. Alternative Assessments

Alternative assessments of pigmentation as well as morphometric assessments of cellular and nuclear sizes and shapes show similar associations with the mutation status of *BRAF* and *NRAS* than variables used in the main analysis (Tables 2 and 3). For ordinal variables the OR is displayed as mean OR per incremental unit. CI is confidence interval.

Found at doi:10.1371/journal.pmed.0050120.st005 (34 KB DOC).

Table S6. Proportion of Misclassified Cases Using Different

Statistical Procedures Using Four Binary Predictions with All (Morphological and Demographic) Variables

Base prediction rate (defined as proportion of the minority class) were 47, 26, 44, and 31% for the entire cohort in each of the four pair-wise comparisons, respectively. Multivariate Logistic Regressions were fit with the variables selected using the single tree (tree) and using the Bayesian information criterion (BIC). The misclassification rate is shown for the entire cohort as well as for samples for which none of the variables are missing. For methods that allow extraction of the independently associated variables those that were found to be significant are shown in the final column.

Found at doi:10.1371/journal.pmed.0050120.st006 (59 KB DOC).

Table S7. Comparison of Features within SSMs by Mutation Status of *BRAF* and *NRAS*

Total percentages that do not add up to 100% have missing values.

Found at doi:10.1371/journal.pmed.0050120.st007 (125 KB DOC).

Table S8. First Metastasis Site

Site of first metastasis in patients who are older and younger than 55 y of age recorded in the Southern German Tumor Registry, with Chi-squared *p*-value analysis showing a significant (<0.0001) difference.

Found at doi:10.1371/journal.pmed.0050120.st008 (29 KB DOC).

Text S1. Detailed Methods for Classification Approaches

Found at doi:10.1371/journal.pmed.0050120.sd002 (29 KB DOC).

Acknowledgments

Author contributions. AV performed the quantitation of the microscopic features and was involved in the project design, statistical analysis, and writing of the manuscript. JF is responsible for the statistical analysis. JB performed sequencing of *BRAF* and *NRAS* in a subset of the samples and was involved in scoring of microscopic features of a subset of the samples. KL and CG performed the statistical analysis of the Southern German Tumor Registry cohort. DP participated in the design of the study and the writing of the manuscript. BCB oversaw the entire project and was involved in the overall project design, data analysis, and writing of the manuscript.

References

1. LeBoit PE, Burg G, Weedon D, Sarasin A (2006) Skin tumours. Pathology and genetics. Lyon (France): IARCPress.
2. Clark WH, From L, Bernadino EA, Mihm MC (1969) The histogenesis and biological behaviour of pimary human malignant melanoma. Am J Pathol 55: 39–52.
3. McGovern VJ, Mihm MC Jr., Bailly C, Booth JC, Clark WH Jr., et al. (1973) The classification of malignant melanoma and its histologic reporting. Cancer 32: 1446–1457.
4. McGovern VJ, Cochran AJ, Van der Esch EP, Little JH, MacLennan R (1986) The classification of malignant melanoma, its histological reporting and registration: a revision of the 1972 Sydney classification. Pathology 18: 12–21.
5. Balch CM, Buzaid AC, Atkins MB, Cascinelli N, Coit DG, et al. (2000) A new American Joint Committee on Cancer staging system for cutaneous melanoma. Cancer 88: 1484–1491.
6. Weyers W, Euler M, Diaz-Cascajo C, Schill WB, Bonczkowitz M (1999) Classification of cutaneous malignant melanoma: a reassessment of histopathologic criteria for the distinction of different types. Cancer 86: 288–299.
7. Ackerman AB, David KM (1986) A unifying concept of malignant melanoma: biologic aspects. Hum Pathol 17: 438–440.
8. Heenan PJ (2003) Nodular melanoma is not a distinct entity. Arch Dermatol 139: 387; author reply 387–388.
9. Bastian BC, Kashani-Sabet M, Hamm H, Godfrey T, Moore DH, et al. (2000) Gene amplifications characterize acral melanoma and permit the detection of occult tumor cells in the surrounding skin. Cancer Res 60: 1968–1973.
10. Bastian BC, Olshen A, LeBoit PE, Pinkel D (2003) Classification of melanocytic tumors by DNA copy number changes. Am J Pathol 163: 1765–1770.
11. Maldonado JL, Fridlyand J, Patel H, Jain AN, Busam K, et al. (2003) Determinants of BRAF mutations in primary melanomas. J Natl Cancer Inst 95: 1878–1880.
12. Curtin JA, Fridlyand J, Kageshita T, Patel HN, Busam KJ, et al. (2005) Distinct sets of genetic alterations in melanoma. N Engl J Med 353: 2135–2147.
13. Curtin JA, Busam K, Pinkel D, Bastian BC (2006) Somatic activation of KIT in distinct subtypes of melanoma. J Clin Oncol 24: 4340–4346.
14. Whiteman DC, Watt P, Purdie DM, Hughes MC, Hayward NK, et al. (2003) Melanocytic nevi, solar keratoses, and divergent pathways to cutaneous melanoma. J Natl Cancer Inst 95: 806–812.
15. Berwick M, Armstrong BK, Ben-Porat L, Fine J, Kricker A, et al. (2005) Sun exposure and mortality from melanoma. J Natl Cancer Inst 97: 195–199.
16. Landi MT, Bauer J, Pfeiffer RM, Elder DE, Hulley B, et al. (2006) MC1R germline variants confer risk for BRAF-mutant melanoma. Science 313: 521–522.
17. Bastian BC, LeBoit PE, Hamm H, Brocker EB, Pinkel D (1998) Chromosomal gains and losses in primary cutaneous melanomas detected by comparative genomic hybridization. Cancer Res 58: 2170–2175.
18. Mihm MC Jr., Clark WH Jr., Reed RJ (1975) The clinical diagnosis of malignant melanoma. Semin Oncol 2: 105–118.
19. Guerry DT, Synnestvedt M, Elder DE, Schultz D (1993) Lessons from tumor progression: the invasive radial growth phase of melanoma is common, incapable of metastasis, and indolent. J Invest Dermatol 100: 342S–345S.
20. Spatz A, Cook MG, Elder DE, Piepkorn M, Ruiter DJ, et al. (2003) Interobserver reproducibility of ulceration assessment in primary cutaneous melanomas. Eur J Cancer 39: 1861–1865.
21. Breslow A (1970) Thickness, cross-sectional areas and depth of invasion in the prognosis of cutaneous melanoma. Ann Surg 172: 902–909.
22. Breiman L, Friedman JH, Olshen R, Stone CJ (1984) Classification and regresssion trees. Monterey (California): Wadsworth.
23. Breiman L (2001) Random forests. Machine Learning 45: 5–32.
24. Landis JR, Koch GG (1977) The measurement of observer agreement for categorical data. Biometrics 33: 159–174.
25. Breiman L (1996) Bagging predictors. Machine Learning 24: 123–140.
26. Lasithiotakis KG, Leiter U, Eigentler T, Breuninger H, Metzler G, et al. (2007) Improvement of overall survival of patients with cutaneous melanoma in Germany, 1976–2001: which factors contributed? Cancer 109: 1174–1182.
27. Garraway LA, Widlund HR, Rubin MA, Getz G, Berger AJ, et al. (2005) Integrative genomic analyses identify MITF as a lineage survival oncogene amplified in malignant melanoma. Nature 436: 117–122.
28. Liu W, Kelly JW, Trivett M, Murray WK, Dowling JP, et al. (2007) Distinct clinical and pathological features are associated with the BRAF (T1799A(V600E)) mutation in primary melanoma. J Invest Dermatol 127: 900–905.
29. Pollock PM, Harper UL, Hansen KS, Yudt LM, Stark M, et al. (2002) High frequency of BRAF mutations in nevi. Nat Genet 25: 25.
30. Shinozaki M, Fujimoto A, Morton DL, Hoon DS (2004) Incidence of BRAF oncogene mutation and clinical relevance for primary cutaneous melanomas. Clin Cancer Res 10: 1753–1757.
31. Kumar R, Angelini S, Hemminki K (2003) Activating BRAF and N-Ras mutations in sporadic primary melanomas: an inverse association with allelic loss on chromosome 9. Oncogene 22: 9217–9224.
32. Omholt K, Platz A, Kanter L, Ringborg U, Hansson J (2003) NRAS and BRAF mutations arise early during melanoma pathogenesis and are preserved throughout tumor progression. Clin Cancer Res 9: 6483–6488.
33. Akslen LA, Angelini S, Straume O, Bachmann IM, Molven A, et al. (2005) BRAF and NRAS mutations are frequent in nodular melanoma but are not associated with tumor cell proliferation or patient survival. J Invest Dermatol 125: 312–317.
34. Edlundh-Rose E, Egyhazi S, Omholt K, Mansson-Brahme E, Platz A, et al. (2006) NRAS and BRAF mutations in melanoma tumours in relation to clinical characteristics: a study based on mutation screening by pyrosequencing. Melanoma Res 16: 471–478.
35. Chang DZ, Panageas KS, Osman I, Polsky D, Busam K, et al. (2004) Clinical significance of BRAF mutations in metastatic melanoma. J Transl Med 2: 46.
36. Kumar R, Angelini S, Czene K, Sauroja I, Hahka-Kemppinen M, et al. (2003) BRAF mutations in metastatic melanoma: a possible association with clinical outcome. Clin Cancer Res 9: 3362–3368.

Editors' Summary

Background. Skin cancers—the most commonly diagnosed cancers worldwide—are usually caused by exposure to ultraviolet (UV) radiation in sunlight. UV radiation damages the DNA in skin cells and can introduce permanent genetic changes (mutations) into the skin cells that allow them to divide uncontrollably to form a tumor, a disorganized mass of cells. Because there are many different cell types in the skin, there are many types of skin cancer. The most dangerous type—melanoma—develops when genetic changes occur in melanocytes, the cells that produce the skin pigment melanin. Although only 4% of skin cancers are melanomas, 80% of skin cancer deaths are caused by melanomas. The first signs of a melanoma are often a change in the appearance or size of a mole (a pigmented skin blemish that is also called a nevus) or a newly arising pigmented lesion that looks different from the other moles (an "ugly duckling"). If this early sign is noticed and the melanoma is diagnosed before it has spread from the skin into other parts of the body, surgery can sometimes provide a cure. But, for more advanced melanomas, the outlook is generally poor. Although radiation therapy, chemotherapy, or immunotherapy (drugs that stimulate the immune system to kill the cancer cells) can prolong the life expectancy of some patients, these treatments often fail to remove all of the cancer cells.

Why Was This Study Done? Now, however, scientists have identified some of the genetic alterations that cause melanoma. For example, they know that many melanomas carry mutations in either the *BRAF* gene or the *NRAS* gene, and that the proteins made from these mutated genes ("oncogenes") help cancer cells to grow uncontrollably. The hope is that targeted drugs designed to block the activity of oncogenic *BRAF* or *NRAS* might stop the growth of those melanomas that make these altered proteins. But how can the patients with these specific tumors be identified in the clinic? The expression of altered proteins is likely to affect the microscopic growth patterns ("histomorphology") of melanomas. However, the current histomorphology-based classification system for melanomas, which distinguishes four main types of melanoma, does not help clinicians choose the best treatment for their patients. In this study, the researchers have tried to improve melanoma classification by looking for correlations between histomorphological features and genetic alterations in a large collection of melanomas.

What Did the Researchers Do and Find? The researchers examined several histomorphological features in more than 300 melanoma samples and used statistical methods to correlate these features with the mutation status of *BRAF* and *NRAS* in the tumors. They found that some individual histomorphological features were strongly associated with the *BRAF* (but not the *NRAS*) mutation status of the tumors. For example, melanomas with *BRAF* mutations had more melanocytes in the upper layers of the epidermis (the outermost layer of the skin) than did those without *BRAF* mutations (melanocytes usually live at the bottom of the epidermis). Then, by combining several individual histomorphological features, the researchers built a model that correctly predicted the *BRAF* mutation status of more than 90% of the melanomas. They also found that, among the variables routinely recorded in cancer registries, being younger than 55 years old was the single most predictive factor for *BRAF* mutations. Finally, in another large group of patients with melanoma, the researchers found that those patients predicted to have a *BRAF* mutation on the basis of their age survived longer than those patients predicted not to have a *BRAF* mutation using the same criterion.

What Do These Findings Mean? These findings suggest that an improved classification of melanomas that combines an analysis of known genetic factors with histomorphological features might divide melanomas into subgroups that are likely to differ in terms of their clinical outcome and responses to targeted therapies when they become available. Additional studies are needed to investigate whether the histomorphological features identified here can be readily assessed in clinical settings and whether different observers will agree on the scoring of these features. The classification model defined by the researchers also needs to be validated and refined in independent groups of patients. Nevertheless, these findings represent an important first step toward helping clinicians improve outcomes for patients with melanoma.

Additional Information. Please access these Web sites via the online version of this summary at http://dx.doi.org/10.1371/journal.pmed.0050120.

- A related *PLoS Medicine* Research in Translation article is available
- The MedlinePlus encyclopedia provides information for patients about melanoma
- The US National Cancer Institute provides information for patients and health professionals about melanoma (in English and Spanish)
- Cancer Research UK also provides detailed information about the causes, diagnosis, and treatment of melanoma